Geo-morphological mapping of the basin configuration of parts of southern Nupe Basin, Nigeria, using high resolution aeromagnetic and core drill dataset

Ayatu Ojonugwa Usman [1*], Ifeanyi Augustine Chinwuko [2] , George-Best Azuoko[1] , Amobi Chigozie Ekwe [1],
Ema Michael Abraham [1] and Joshua Chima Chizoba[1]

[1] *Alex Ekwueme Federal University, Department of Geology/Geophysics, Ndufu-Alike, Ebonyi, Nigeria*
[2] *Nnamdi Azikiwe University, Department of Applied Geophysics, Awka, Nigeria*

Abstract

Aeromagnetic and core drilled data covering parts of southern Nupe Basin was acquired and interpreted with the view of evaluating the mineral potential of the area through interpretation of the structural features in the area, determination of the Curie isotherm depth, and correlation of aeromagnetic outcomes with the core sample data from the area. Two major regional fault trends were interpreted: northeast–southwest (NE–SW) and NNE–SSW with minor northwest–southeast (NW–SE) directions. Two depth sources in the area are delineated, namely zone of shallow seated basement which ranges from 0.42 km to 1.5 km and zone of deeply seated basement ranging from 1.91 to 3.50 km. Results of qualitative interpretation of the total magnetic intensity map (TMI) and residual intensity map reveal that the magnetic intensities range from 7500 to 8460 nano-Tesla (nT) and -220 to 240 nT, respectively. The depths to the centroid and top of the magnetic causative bodies range from 9.00 to 17.10 km and 0.4 to 3.10 km, respectively. There are evidences of oolitic iron ore in some parts of the study area. Juxtaposing the topographical and core drilling data reveal that the oolitic iron ore level follows the topographical level which implies that the topography of the area controls the configuration of the iron ore deposit level. All these deductions are made considering the geology of the area.

Keywords: Basin geometry, core data, spectral analysis, Curie isotherm, oolitic Iron ore

*Corresponding author: ayatu.ao@funai.edu.ng

1   Introduction

Magnetic prospecting method can be used to investigate subsurface geologic structure by delineating rocks and minerals with unusual properties which reveal themselves in the form of anomalies. These anomalies are normally produced by magnetic susceptibility variations of the underlying rocks (Bemsen et al., 2023). Deeply seated magnetic rocks typically exhibit differences in the earth's geomagnetic field from anomalous magnetic structures. Although certain rock types have appreciable magnetic minerals (mostly magnetite) to form recognizable anomalous magnetic bodies, a majority of rock forming minerals are non-magnetic and almost all have small to very low magnetic susceptibilities. Sedimentary rocks generally contain low magnetic susceptibility values, whereas crystalline rocks (basement igneous and metamorphic rocks) have the high magnetic susceptibility values (Abraham et al., 2022).

The use of spectral analysis to estimate basal depth is a powerful tool for quantitative studying of space data (Singh and Biswas, 2016). The present research aimed at the delineation the basin configuration through spectral analysis of the aeromagnetic data with a view of delineating the basal morphology of the area. Aeromagnetic surveys routinely target causative magnetic bodies that produce unusual anomalies. Strong magnetic anomalies are predominantly in basement rocks and mostly minimal in sedimentary rocks. According to Onwuemesi (1995, 1997) and Anakwuba and Chinwuko (2015), delineation of the subsurface requires a more advanced technique which the magnetic survey provides. This technique is a fast, target-oriented, and cost-effective geophysical method that can help map subsurface structures, calculate source depth parameters, and model source bodies such as exploration for solid minerals.

The work of Abraham et al. (2022) on mapping of mineral deposits within granitic rocks by aeromagnetic data—a case study from Northern Nigeria, clearly shows the efficacy of using aeromagnetic data in delineating structures that controls mineralization in an area. The study of Ojonugwa et al. (2018) shows the application of spectral analysis in evaluation of the basin configuration of an area. This work aims at employing similar method in delineating the basal morphology of the area.

The work of some notable authors such as Bhattacharyya and Leu (1975), Ross et al. (2006), Mandal et al. (2013), Abraham et al. (2014), Saibi et al. (2015), and Singh and Biswas (2016) suggest that the Curie isotherm and geothermal gradients can be used as useful indictors for mineral prospecting. This study integrates aeromagnetic and core dataset to evaluate the mineral potential of the basin.

We evaluate the mineral potential of the Nupe Basin through the use of centroid and forward modelling of the spectral peaks, over some parts of Southern Nupe Basin, North Central Nigeria. This will delineate the geometry of the basin by evaluating the depth to top of the causative magnetic source rocks, the thickness of the magnetic basement, and crustal temperature information in the area of study. It will also reveal the geologic structures and provides a 3D model of the basin

2   Location and geology of the area

The study area is situated within the Nupe Basin, also called the Mid Niger Basin. It lies between latitudes 8°00′N- 9°30′N and longitudes 5°30′E- 7°00′E (Figure 1) and some noted towns there include Bida, Paiko, Pategi, Baro, Gulu, Isanlu, Aiyegunle, Kotonkarfi and BirinIt. It is an intracratonic basin extending from Kontagora in Niger State to areas slightly beyond Lokoja in the south (Obaje et al., 2013) (Figures. 2 and 3). The study area was chosen because of its interesting features such as sedimentary/basement contact, high
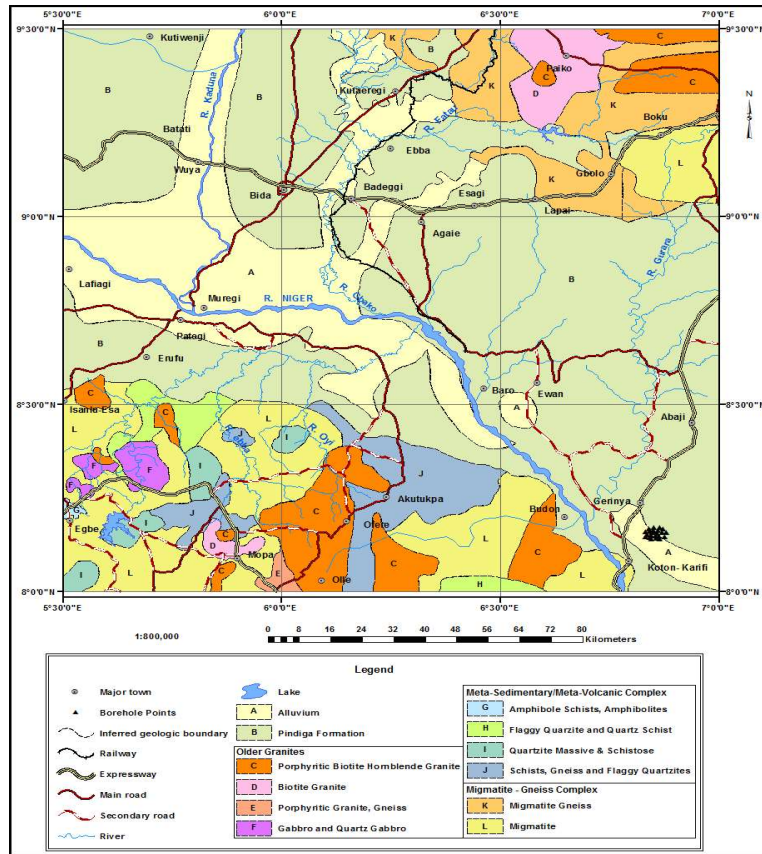
level

Figure 1. Location and geological setting of the study area.
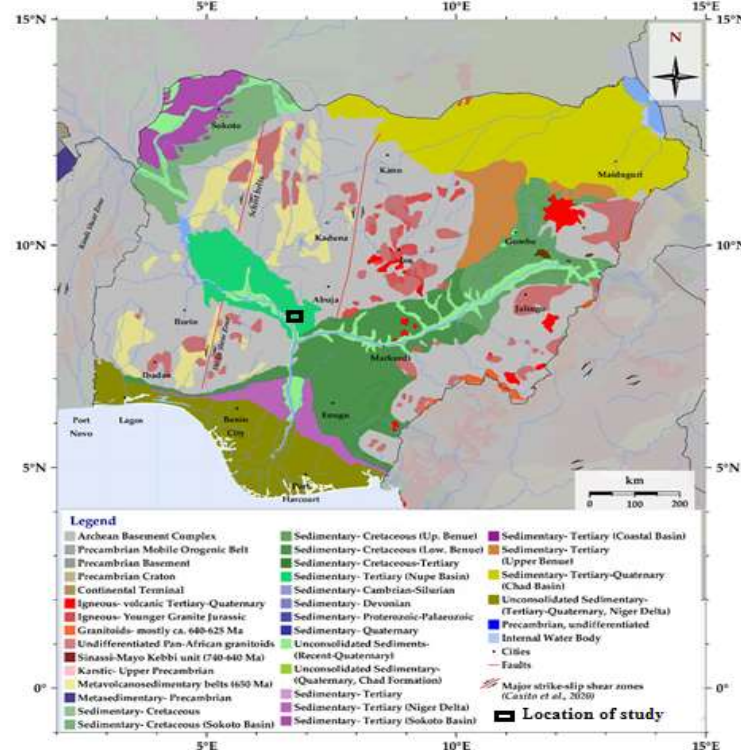

Figure 2. Location of study area in the geologic map of Nigeria (After Obaje et al., 2013).
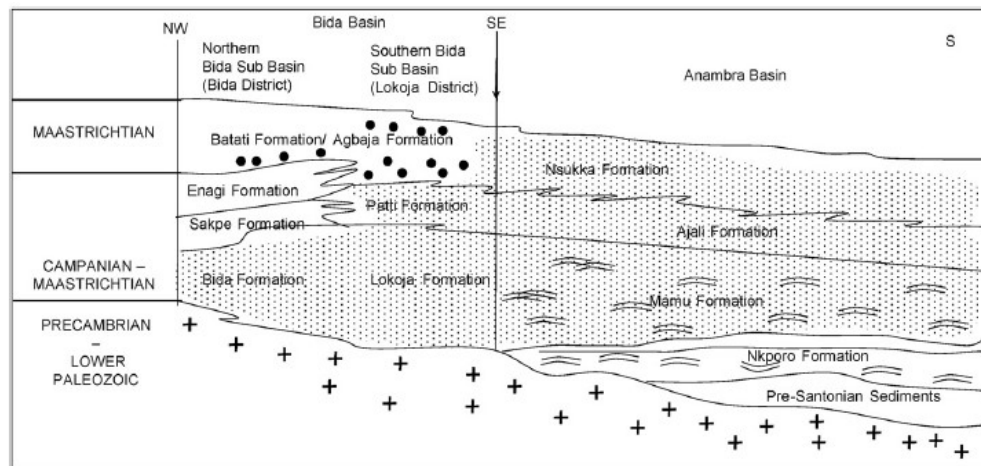
Figure 3. The formation of Southern Nupe Basin correlated with Anambra Basin (modified from Akande et al., 2005).

geological structures and evidences of mineralization.

The stratigraphic sequence of the Nupe Basin is referred to as the Bida Group (Adeleye, 1974). It is subdivided into Northern Nupe Sub-Basin and Southern Nupe Sub-Basin or Lokoja Sub-Basin (Figure 2). The Nupe Basin is presumed to be a northwestern extension of the Anambra Basin (Akande et al., 2005). The basin fill contains Cretaceous sediments that were believed to be deposited as a result of subsidence, rifting, block faulting, basement fragmentation and drifting resulting from the Cretaceous opening of the South Atlantic Ocean. The main parallel lateral movements of the northeastern to southwestern axis of the adjacent Benue Trough occurred in early Cretaceous time have been interpreted as the north-south and northwest trending shear regions that form the Nupe Basin that abrupt to the Benue Trough (Ojonugwa et al., 2018).

Nupe Basin is an extension of the Anambra Basin but it was subdivided in the Santonian. There is an accumulation of Pre-Santonian sediment in the lower Benue Trough and the adjacent southern Anambra Basin. Obaje et al. (2013) recorded that the Nupe Basin and the Southern Anambra Basin platforms collapsed and this led to sedimentation of the upper

Cretaceous depositional cycle which was begun with the accumulation of the marine shales (the Nkporo shale and Enugu shale Formations). These formations are believed to have some lateral equivalent with the Lokoja Formation of the Nupe Basin (Obaje et al., 2013).

The Mamu Formation of the Southern Anambra Basin underlies the Nkporo shale Formation. Lithologically the Mamu Formation comprises of sandstone, siltstone with shale intercalation and coal seam deposits of deltaic to estuarine environments. Its lateral equivalent is the Bida Formation in the Nupe Basin (Obaje et al. 2013). The Ajali Sandstone Formation underlies the Mamu Formation and its lateral equivalents are the Patti, Sakpe and Enagi Formations of the Nupe Basin (Figure 3). The predominant lithic component of this formation is well sorted sandstone. This sandstone is commonly interbeded with claystone and siltstone. This is eminent in Patti Formation. Agbaja Iron Formation and Batati Formation are iron rich. They overlie the Patti and Batati Formations (Figure 3). The Ajali Sandstone Formation is rich in iron deposit and structurally aligned.

3   Methodology

The input data used in the study are nine aeromagnetic datasets, namely sheets 183 (Egbako), 184 (Bida), 185 (Paiko), 204 (Pategi), 246 (Baro), 206 (Gulu), 225 (Isanlu), 226 (Aiyegunle) and 227 (Koton-karfi) and core drilled around Koton-Karfi area. The aeromagnetic sheets were assembled, analysed and digitised on a scale of 1:100,000 for a total surveyed area of 27,225 km^2. The input data used for the spectral analysis is the residual data which helps in evaluation of depth to the magnetic sources and delineation of Curie isotherm temperature and heat flow. Hence, the residual data were subjected to both graphical and mathematical modelling for quantitative interpretation. This helps us to deduce the thermomagnetic properties which will help in the mineral evaluation in the area. The aeromagnetic data were also enhanced using mathematical filters such as downward continuation, upward continuation, first vertical derivative, analytical signal and reduction to the pole. To interpret the prevailing magnetic anomalous body, the data is separated into regional field and residual field using the multiple regression techniques.

Aeromagnetic data were obtained as part of a national aeromagnetic survey sponsored by the Geological Survey of Nigeria. Data are collected along a series of NW-SE trajectories spaced at 2 km intervals, with mean flight altitudes of approximately 150 m and tie lines occurring at approximately 20 km intervals. Geomagnetic gradients were removed from the data using the International Geomagnetic Reference Field (IGRF).

The borehole data is obtained from the Enegbaki-Akpogu oolitic iron ore deposit situated about 9 km north-east of Akpogu village along Lokoja-Abuja Road. The deposit investigated has an area of 1.0 km^2 and is capped by a lateritic layer, clay and some silica. The iron-ore bearing plateau trends in a NE–SW direction with an average height of 263 m above sea level. Twenty-five (25) core holes placed at a 250 m grid interval were drilled using a rotary type of drilling (Massenza multi-purpose drill).

Qualitative interpretations were done using visual inspection of the total magnetic field data, residual field data and analytical signal map of the area. Core data were analysed and interpreted in order to produce the oolitic iron model in the area. Lastly, areas with geothermal energy potential were delineated using integrated geological and geophysical data. The workflow is shown in Figure 4-b.

4 Background of spectral analysis and Peter's half-slope methods

Bhattacharyya and Leu (1975) method was adopted for the spectral analysis of the aeromagnetic data. According to this method, the first step was to estimate the depth to centroid (Z_o) of the magnetic source from the slope of the longest wavelength of the spectrum:

$$ln\left[\frac{P(\sqrt{S})}{/S/}\right] = lnA - 2\pi/S/Z_o \qquad (1)$$

where P(s) is the radially averaged power spectrum (natural log of amplitude) of the anomaly, /s/ is the wave number (Nyquist frequency) and A is a constant.

The second step is the estimation of the depth to the top boundary (Z_t) of that magnetic source from the slope of the second longest wavelength spectral segment (Okubo et al., 1985):

$$ln\left[\frac{P(\sqrt{S})}{/S/}\right] = lnB - 2\pi/S/Z_t \qquad (2)$$

where B is the sum of constants. It is independent of /s/.

Then, the basal depth (Z_b) of the magnetic source was calculated from the equation of Bhattacharyya and Leu (1975) as shown below (Biswas et al., 2017):

$$Z_b = 2Z_o - Z_t \qquad (3)$$

The obtained basal depth (Z_b) of magnetic sources in the study area is assumed to be the Curie point depth according to Biswas and Acharya (2016) and Bhattacharyya and Leu (1975).
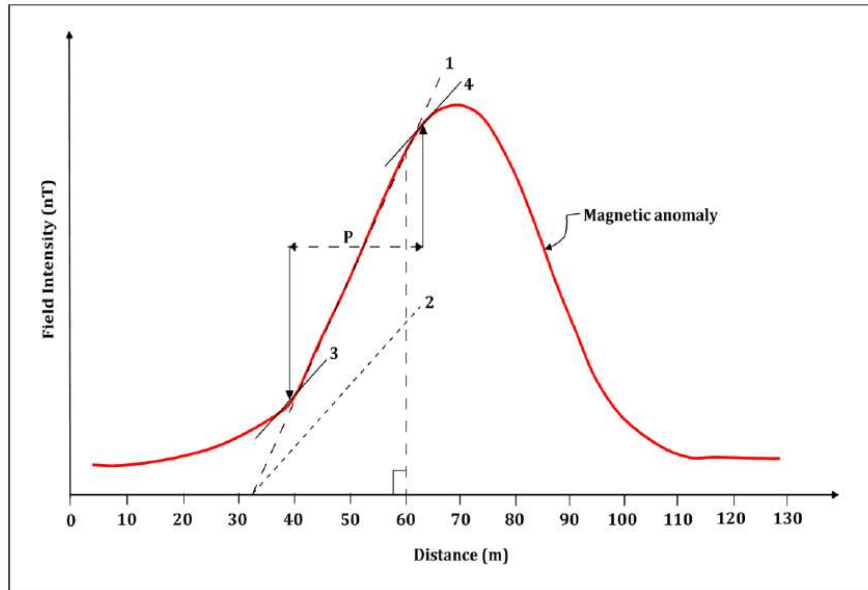
(a)
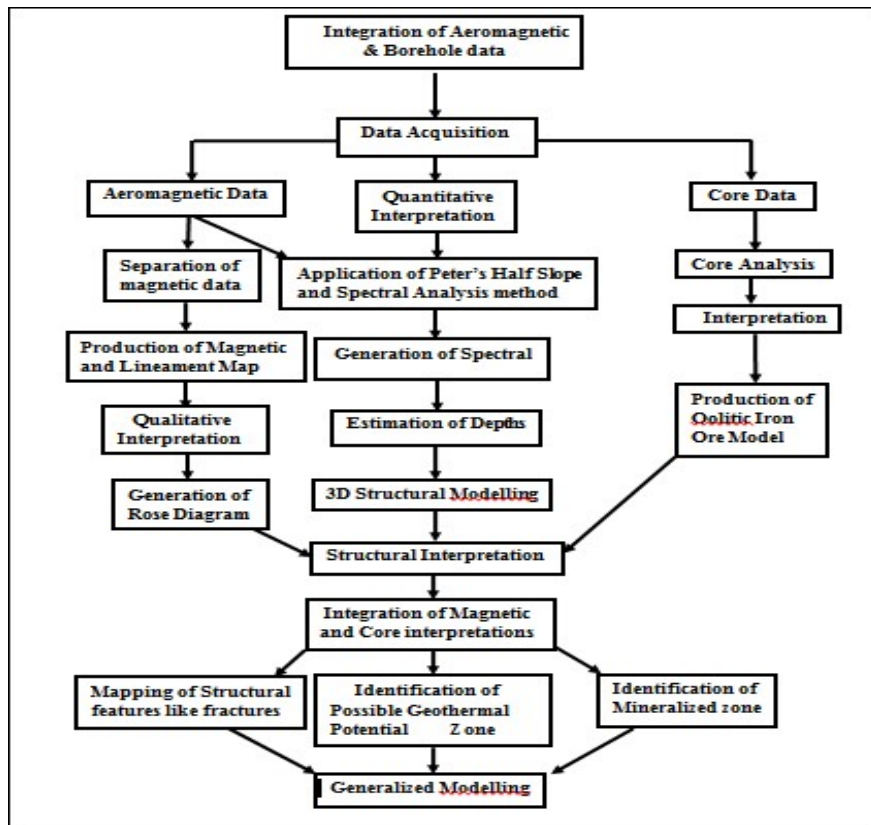
(b)

Figure 4. (a) Peter's half-slope method of depth determination [modified after Ojonugwa et al. (2018)].(b) Research workflow.

The obtained basal depth (Z_b) of magnetic sources in the study area is assumed to be the Curie point depth according to Biswas and Acharya (2016) and Bhattacharyya and Leu (1975).

Next, the heat flow and thermal gradient values were calculated in the study area using an equation expressed by Fourier's law as follows:

$$q = \lambda \frac{dT}{dZ} \tag{4}$$

where q is the heat flow and λ is the coefficient of thermal conductivity.

According to Tanaka et al. (1999), the thermal gradient (dT/dZ) can be estimated using Eq. (5), where we have the Curie temperature (θ) and the Curie point depth (Z_b) available:

$$\theta = \left[\frac{dT}{dZ}\right] Z_b \tag{5}$$

Peter's rule is based on arithmetical expression for magnetic anomalies over vertical dykes with vertical polarization (Chinwuko et al., 2013; Ojo et al., 2014). The application of this method requires the proper identification and location of the point of maximum amplitude on the slope of a magnetic anomaly chart (Figure 4-a). According to Ojo et al. (2014), the magnetic body is then assigned a specific index value or proportionality factor ranging from about 1.2 to 2, depending on the objects size. The depth of the object is then obtained by dividing the horizontal distance by the index value. For this study, the depth to the magnetic body is given as:

$$h = 1.6p \tag{6}$$

5 Results and Discussion

The total magnetic intensity (TMI) and residual anomaly maps (Figures. 5 and 6) were contoured from the digitized data. Visual assessment of the TMI and residual anomalous maps reveals intricate form of magnetic signatures of both short and long wavelengths (Figures. 5 and 6). This is an indication of variable magnetic intensities from diverse geologic sources as supported by the work of Okonkwo et al. (2012). These variable magnetic intensities are well pronounced in the study area. The mangetic intensity values of the TMI and residual anomalous maps range from 7800 to 8200 nT and -220 to 240 nT, respectively (Figures. 5 and 6). There are strong evidences of igneous intrusion when juxtaposed with the geologic map of the area. These intrusions, the faulting and folding can serve as migrating pathway or house for mineralisation.
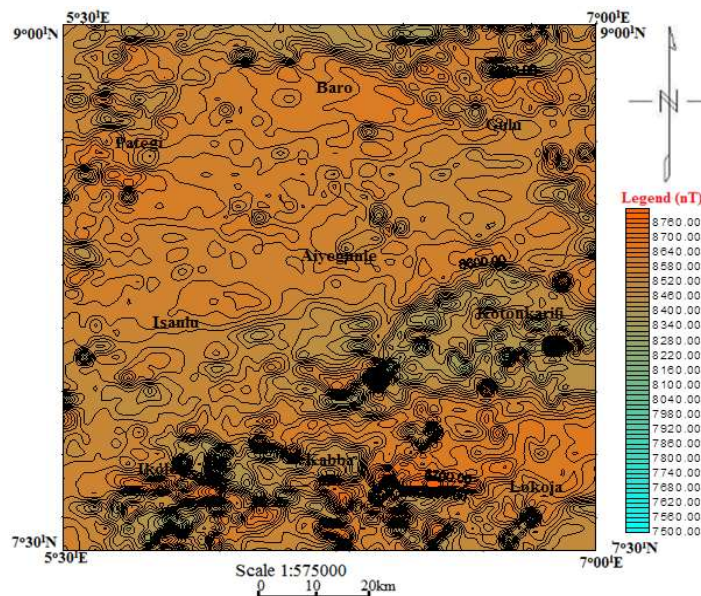

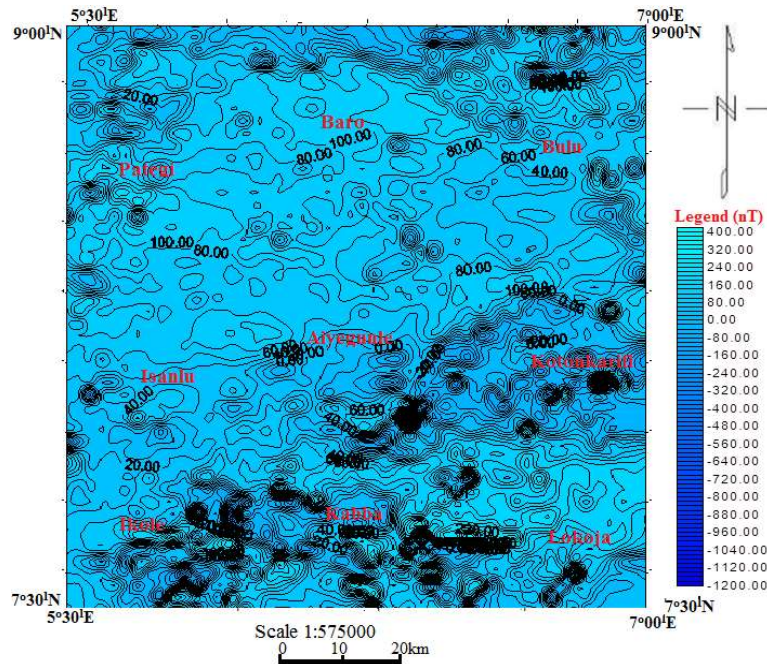**Figure 5**. TMI map of the study area (contour interval~20nT).

Figure 6. Residual map of Bida and its environs (contour interval~20nT).

The areas mentioned above possess mostly sharper gradients and shorter wavelengths. This implies thinner sedimentary infillings (that is the depth to the top of the basement is shallow). Oval contours encountered in this area may also be an indication of intrusive igneous bodies or lineaments containing groups related to the mineral deposit as evident in the study area like Koton-Karfi, Abaji, Bida and Paiko.

The central parts of the study area (Pategi, Baro, Gulu, Lafiagi) contain long wavelengths, signifying thick sedimentary infilling (that is deeper magnetic sources)

within these areas (Figure 5). It is therefore concluded that the short wavelength and sharp gradient have high magnetic intensity values which may relate to a vein bearing mineral. This assertion is supported by the geologic map of the study area (Figures. 3 and 7).

The structural alignment of the area was evaluated using the anomalous residual shaded maps (Figurs. 8 and 9) produced from the residual anomalous field intensity map. The major trend of the lineaments was NE-SW and the minor ones were E-W and NW-SE.
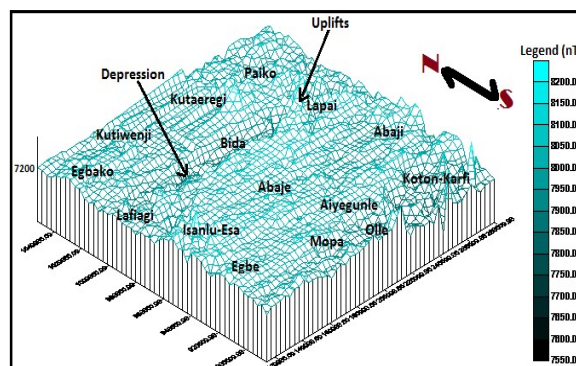

Figure 7. Real view distribution of total magnetic field intensity in the area.
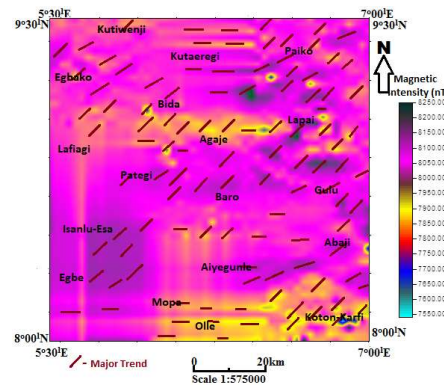
Figure 8. Analytical map of the study the area.

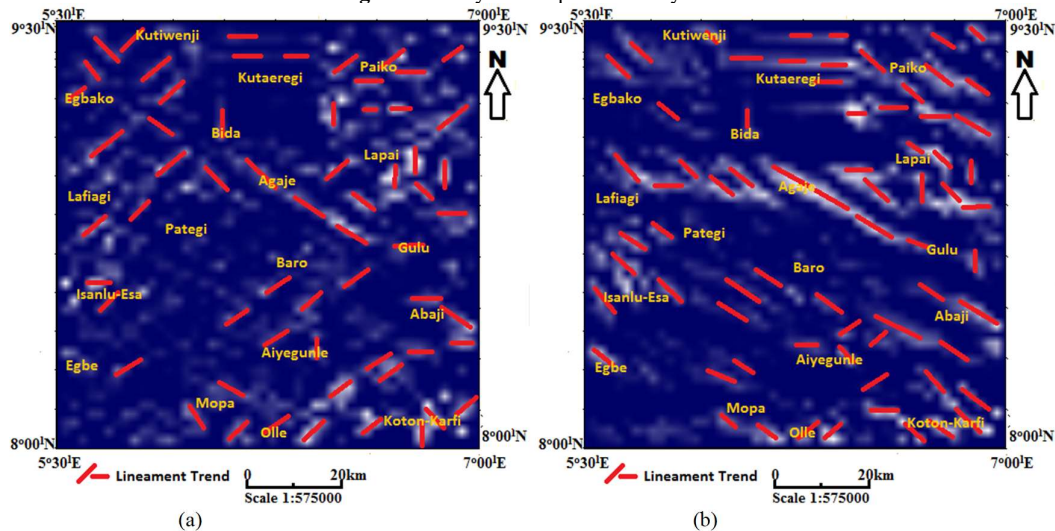(a)   (b)

Figure 9. Residual shaded intensity field maps showing structural direction. (a) HPLA-0° and VPLA-0°. (b) HPLA-45° and VPLA-0° (HPLA: Horizontal Position Light Angle, VPLA: Vertical Position Light Angle).

This structural direction is in conformity with previous studies of Chinwuko et al. (2012, 2014), Ojonugwa et al. (2018), and Olufemi et al. (2020). There is high lineament concentration which suggests intense tectonic activities affect the deeply seated basement rock and abut Cretaceous sequences. Previous works such as Obaje et al. (2013), Abraham et al. (2014) and Ojonugwa et al. (2018) propose that the NE-SW, NNE-SSW and NW-SE lineaments within the study area are regarded as Pan-African Orogeny whiles the E-W may probably have been Pre-Pan-African Orogeny. The structures can serve as migrating path for geothermal and fluid.

The residual magnetic anomalies data were subjected to both Peter's half-slope method and spectral analysis for depth calculation (sedimentary thicknesses) and depth modelling within the study area (Figure 10). The result of the analysis is shown in Table 1. The interpreted result reveals two-layer depth model. The depth of the shallower magnetic bodies varies from 0.54 to 1.87 km using Peter's slope method, and 1.27 to 1.96 km using spectral analysis interpretation. The depth of deeper magnetic bodies ranges from 2.01 to 3.27 km (for Peter's slope method) and 2.01 to 4.27 km for spectral analysis. Again, the depth to the centroid obtained through the spectral analysis reveals depth range of 9.79 to 15.75 km across the area (Table 1).

The magnetic depth calculation result (Table 1) shows that Curie isotherm depth varies from 19.18 to 30.95 km with an average of 23.12 km. Also, the geothermal gradient ranges from 21.98 to 30.95°C/km

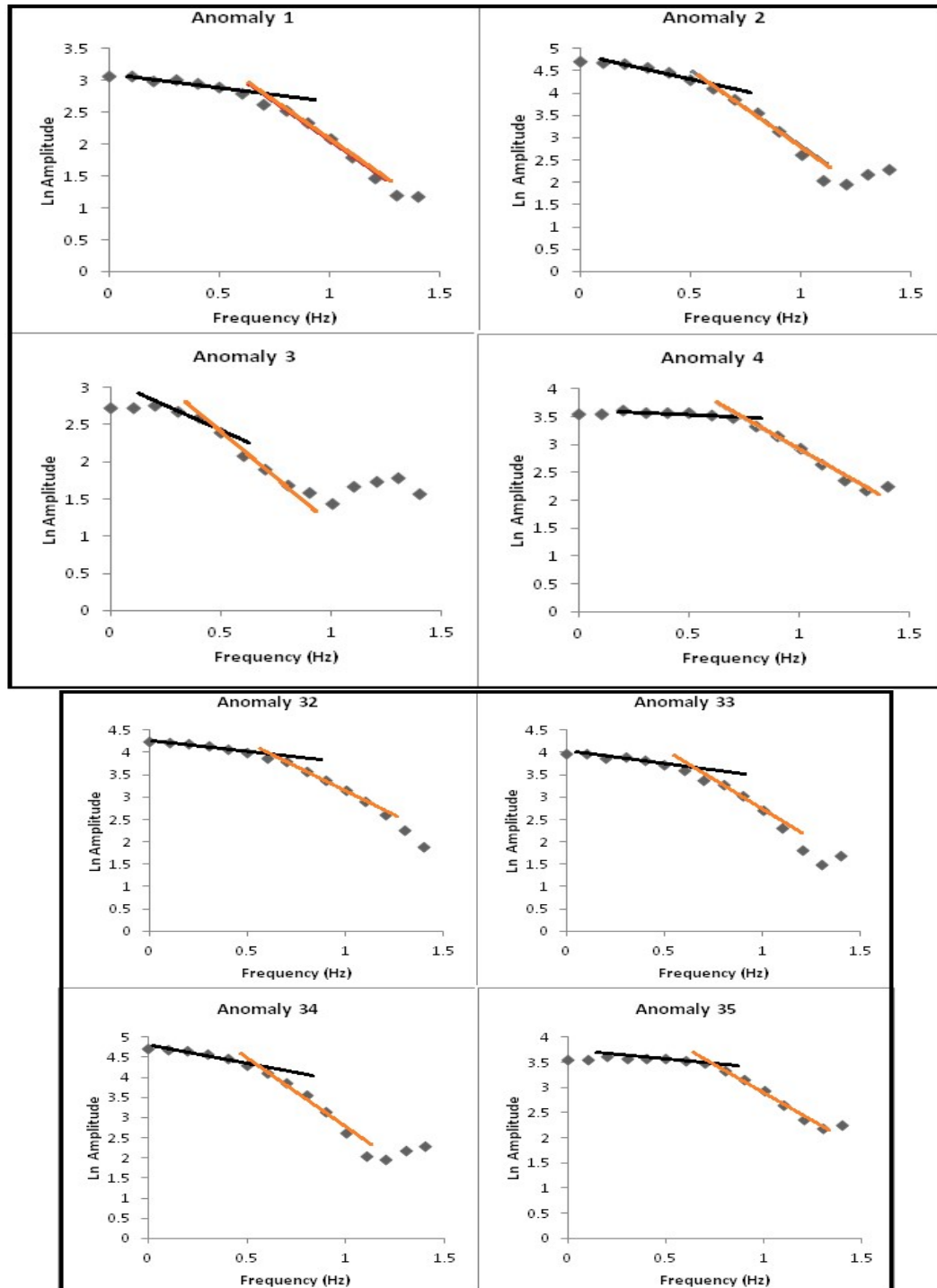**Figure 10.** Representative spectral graph in the area.

with an average of 25.27°C/km and the heat flow (flux) obtained varies from 51.95 to 77.37 mWm^2 with an average of 63.17 mWm^2.

From the depth calculations using spectral analysis, two anomalous depth sources were interpreted. The deeply seated magnetic anomalous sources vary from 1.91 to 3.78 km, and shallower seated magnetic

Table 1. Depth calculation using spectral analysis.

| Anomaly | Spectral analysis | | Peter's slope method | | | |
	Depth to top of basement Z_t (km)	Depth to bottom of basement Z_p (km)	Z_o (km)	Curie point depth (km)	dT/dZ (°C/km)	q (mWm²)
1	2.09	1.86	14.73	27.37	24.733	61.834
2	3.11	2.41	12.84	22.57	28.046	70.116
3	1.49	2.88	15.11	28.73	23.359	58.397
4	0.96	0.56	13.45	25.94	24.380	60.950
5	2.42	2.64	12.88	23.34	28.238	70.594
6	3.18	2.93	10.06	16.94	23.191	57.977
7	3.05	2.71	13.92	24.79	23.800	59.499
8	1.52	1.83	12.87	24.22	26.197	65.492
9	1.14	2.05	14.31	27.48	28.798	71.996
10	1.08	2.61	12.95	24.82	20.781	51.953
11	0.53	2.28	16.28	32.03	25.043	62.608
12	2.46	1.42	12.21	21.96	25.641	64.103
13	3.22	2.33	11.04	18.86	22.516	56.289
14	3.07	2.39	14.53	25.99	23.761	59.402
15	1.49	1.71	16.84	32.19	30.240	75.600
16	0.45	2.14	15.06	29.67	28.087	70.2179
17	2.71	3.27	13.01	23.31	24.545	61.363
18	3.24	1.81	9.09	14.94	26.316	65.789
19	3.19	2.96	11.23	19.27	24.017	60.041
20	2.85	2.57	13.69	24.53	24.618	61.545
21	2.25	1.74	14.47	26.69	24.733	61.834
22	2.33	1.71	12.61	22.89	27.154	67.884
23	2.08	2.01	11.89	21.7	26.839	67.099
24	2.86	2.11	14.05	25.24	24.670	61.676
25	3.23	2.42	13.11	22.99	25.709	64.273
26	2.98	1.72	9.47	15.96	26.902	67.254
27	1.81	1.79	13.22	24.63	22.222	55.556
28	1.65	0.78	16.51	31.37	21.978	54.945
29	2.13	0.83	14.83	27.53	24.278	60.695
30	3.17	2.15	16.32	29.47	24.116	60.291
31	3.22	1.44	11.63	20.04	23.761	59.402
32	2.08	0.76	13.83	25.58	26.364	65.909
33	2.01	1.96	12.94	23.87	30.950	77.375
34	2.14	1.38	15.77	29.4	25.483	63.708
35	2.33	1.97	13.22	24.11	24.744	61.860
36	2.79	2.38	15.64	28.49	23.043	57.608
37	2.47	1.16	14.85	27.23	27.397	68.493
Average	2.29135135	2.01	13.52594595	24.76054054	25.277	63.173
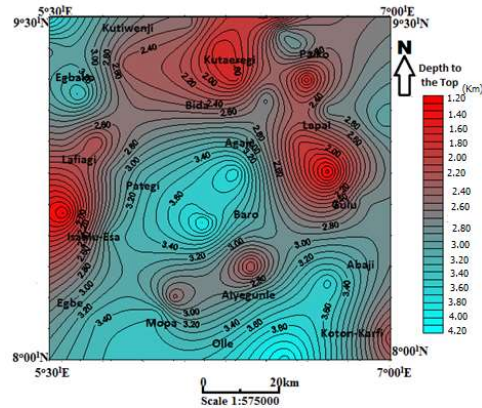
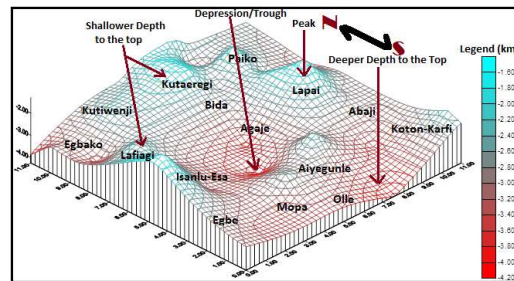**Figure. 11**. Basal depth. Contour interval is ~0.1m.

Figure.12. Real view model of depth to the top in the area.

anomalous sources range from 0.98 to 1.98 km (Figure 11). Deeply seated magnetic anomalous sources may possibly denote depth to the basal crystalline rocks, while the shallower ones maybe associated with intrusive igneous and/or magnetized bodies covered by sediments. The basal depth is abysmal in the entire south and central part of the study area, whereas other parts of the area such as Kutawenji, Lafiaji, Koton-Karfi and Lapai have shallower sources.

The 3-D surface plot of depth to the top of the anomalous magnetic body shows the presence of peaks (uplifts) and depressions (troughs). Around Agaje, Egbako, Olle, Mopa and Abaji areas, there are visible linear depressions. These areas presumably have deeper sediments than the other parts such as Kutaeregi, Paiko, Lapai, Lafiagi, Aiyegunle, and Koton-Karfi areas which have prevalent uplifts (peaks) in conjunction with smaller sedimentary thicknesses (Figure 12).

The presence of these peaks (uplifts)

suggests that there are numerous intrusive bodies around these areas; as a result, there are more tectonic activities in the areas associated with depressional feature. According to Abraham et al. (2022), Biswas (2015) and also Biswas et al. (2016, 2017), these identified igneous intrusives generally occur as sills and dykes (Table 1).

6   Prevalent intrusive sources and geologic model across a profile in the area
The geologic model (Figures. 13 and 14) obtained from the quantitative interpretation of the residual magnetic data reveals four geological stages, namely sedimentary stage, ferromagnetic bodies, paramagnetic bodies and lower crust bodies. The sedimentary infilling along this profile has a variable thickness which ranges from 0.20 to 3.21 km. The deepest sedimentary cover occurs at the eastern and western ends of the profile (Egbe) (Figure 14-a) while the shallowest is at the middle.
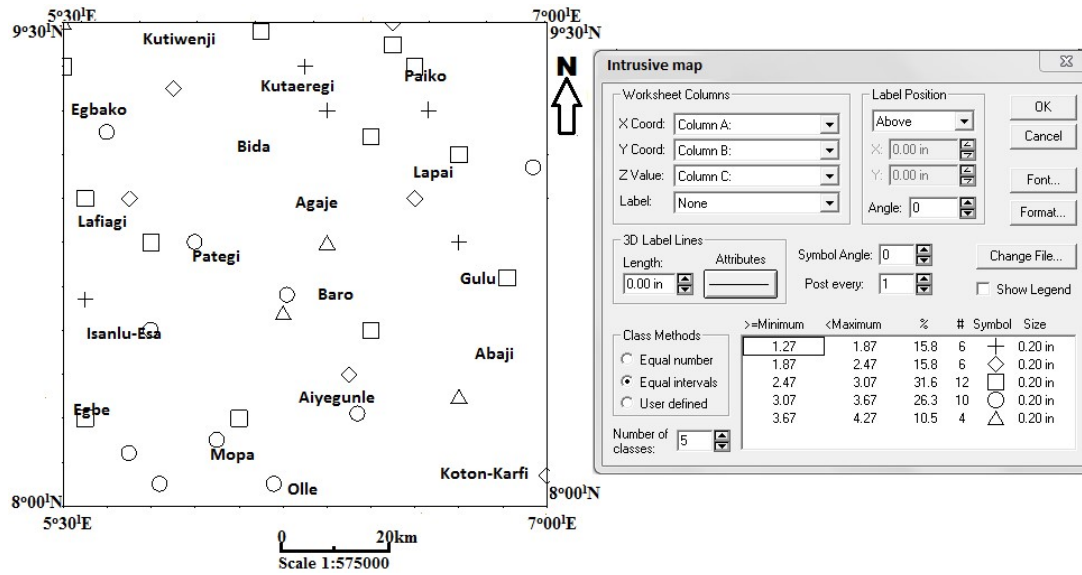
Figure 13. Prevalent intrusive sources in the area.

(a)   (b)
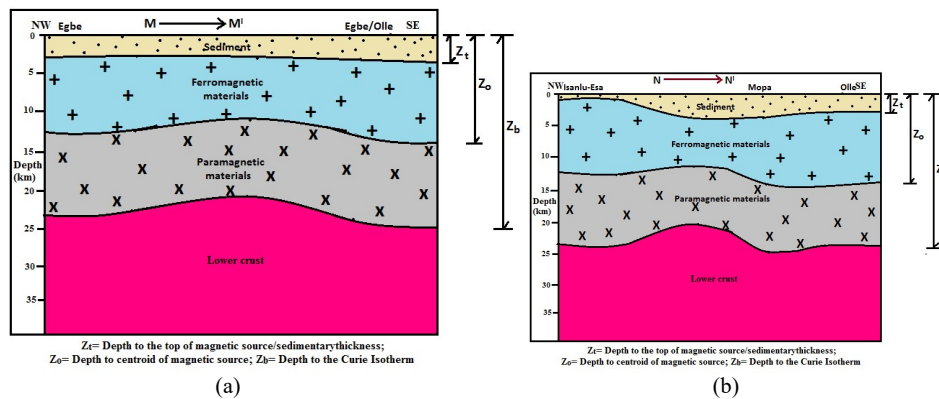
Figure 14. Curie isotherm depth modelling along profiles (a) M-M^1 (b) N-N^1 in the study area.

Moreover, the ferromagnetic bodies underlie the sedimentary layer with an average thickness of 6.1 km. The depth to the ferromagnetic bodies ranges from 12.04 to 13.0 km in this profile. Also, the paramagnetic bodies which are associated with Curie point depths and upper mantle have depth range of 13.10 to 24.01 km. It is believed that the heat from the mantle must have been reworked the magnetic bodies and made them to loss the magnetism (Bemsen et al., 2023; Adewumi et al., 2021). The model suggests that the deepest Curie point depth occurs in both left and right hand side of the model, while at the middle, the Curie point depth is the shallowest. The model interpretation is also shown in Figure 14-b.

7   Core sample analysis and its implication around Koton-Karfi

Core sample analysis within Koton-Karfi reveals different lithologic units within the sample locations. The depth to the oolitic iron ore obtained across the area ranges from 20.79 to 101.2 m with an average of 38.52 m (Table 2).

The elevation map of Koton-Karfi area (Figure 15) was produced for effective correlation with the oolitic iron ore level map (Figure 15). The oolitic iron ore level with respect to mean sea level across Koton-Karfi area was computed by subtracting depths to oolitic iron ore layers deduced from the core drilling from surface elevations obtained during the data acquisition (Table 2). Thus, maps of the oolitic

Table 2. Oolitic iron ore deposit level with respect to mean sea level (MSL).

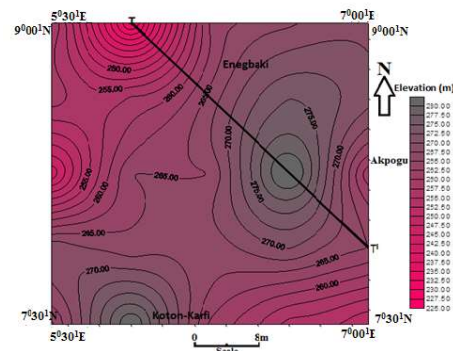| Borehole coordinates	Elevation (m)	Borehole depth (m)	Oolitic ore deposit level w.r.t. MSL (m)
N08°09'30.5" E006050'48.1"	260	42.56	217.44
N08°09'30.5" E006050'48.1"	263	35.2	227.8
N08°09'30.7" E006051'12.6"	267	39.68	227.32
N08°09'30.7" E006051'20.8"	269	42.82	226.18
N08°09'22.3" E006050'48.2"	259	42.65	216.35
N08°09'22.4" E006050'56.4"	258	39.34	218.66
N08°09'22.4" E006051'12.7"	266	39.33	226.67
N08°09'22.7" E006051'20.8"	275	42.38	232.62
N08°09'22.7" E006051'20.8"	271	42.59	228.41
N08°09'14.2" E006050'48.3"	243	42.62	200.38
N08°09'14.9" E006051'04.7"	265	42.37	222.63
N08°09'06.1" E006050'56.4"	266	42.34	223.66
N08°09'06.1" E006051'04.7"	266	40.32	225.68
N08°09'0.63" E006051'12.9"	270	41.61	228.39
N08°09'0.64" E006051'21.1"	265	42.61	222.39
N08°08'58.0" E006050'56.4"	283	40.45	242.55
N08°08'58.1" E006051'04.8"	262	42.61	219.39
N08°08'58.2" E006051'13.1"	254	24.05	229.95
N08°08'58.1" E006051'21.0"	250	20.79	229.21
N08°08'58.0" E006050'48.4"	262	25.53	236.47
N08°09'06.09" E006050'48.3"	270	20.79	249.21
N08°09'14.2" E006051'56.4"	265	23.05	241.95
N08°09'14.3" E006051'12.6"	284	23.05	260.95
N08°09'14.5" E006051'21.1"	258	23.05	234.95
N08°09'30.6" E006050'56.2"	229	101.2	127.8
Average	263.20	38.52	224.68

Figure 15. Elevation map of Koton-Karfi area. Contour interval is ~2.5 m.
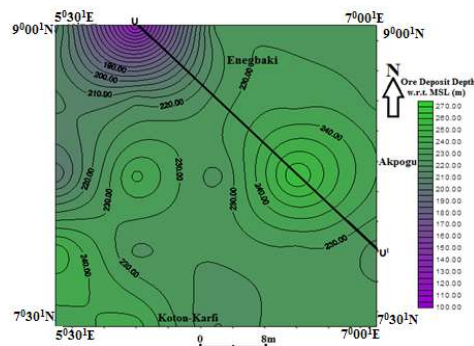
Figure 16. Oolitic iron ore level of Koton-Karfi area. Contour interval is ~5 m.

iron ore levels with respect to elevations were generated in order to evaluate the possible trend of the oolitic iron ore level across the study area (Figure 16). Considering elevation and oolitic iron ore maps of Koton-Karfi area (Figures. 15 and 16), it is evident mineralogically that the trend of the oolitic iron ore level is predominantly in NE-SW direction.

Result from the core drill data reveals that the anomalous body level (ooilitic iron ore level) is deep around northeastern and south-western parts of Koton-Karfi, whereas at northwestern part of Koton-Karfi, the depth to the anomalous body (ooilitic iron ore) is shallow with average oolitic iron ore deposit level as 225 m.

Furthermore, profiles running from T-T^l at Figure 14 and U-U^l at Figure 15 were superimposed in order to establish the variation phenomenon across the area. Here, it was observed that the oolitic iron ore level follows the topographical level which implies that the topography controls

the configuration of the iron ore level (Figure 17).

Result from qualitative interpretation reveals that the area is extremely fractured, with fractures trending NE-SW direction and minor ones in NW-SE and E-W directions. The trend of these structures is in conformity with the trend of structures within the Nupe Basin. These fractures can serve as migrating pathway for both geothermal energy flow and fluids like hydrocarbon. The work of Ojonugwa et al. (2018) believes that the stratified nature of the carbonaceous shale with intercalated sandstone found within the study area may probably favour fluid migration into potential reservoir rocks that are made up mostly of fluvial deposit, flood plain and shelf sandstones of the Lokoja and the Patti Formations.

Quantitatively, the depth to the top of magnetic basement rock (sedimentary thickness) within the study area has been delineated along seven different profile lines using Peter's half slope and spectral

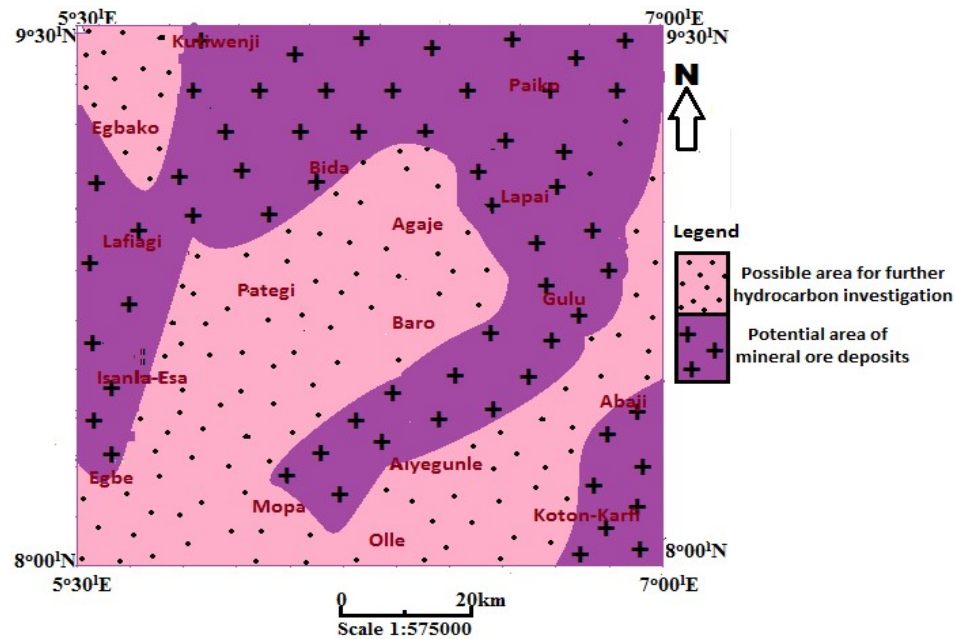**Figure 17.** Juxtaposed topography and oolitic ore deposit level of Koton-Karfi area.

analysis of aeromagnetic data. The result shows two depth model across the area, namely the shallower magnetic sources which vary from 0.56 to 1.96 km and the deeper magnetic sources which vary from 2.01 to 4.27 km. The Curie isotherm depth result revealed deeper depth at Kutiwenji, Egbako, Lapai, Paiko, Olle, Mapo and Baro areas, ranging from 22.60 to 27.91 km. In other parts, the Curie isotherm depth was shallower and ranged from 19.18 to 22.20 km. The calculated thermomagnetic properties reveal average values of 23.12 km Curie isotherm depth, 25.27°C/km geothermal gradients and 63.17 mWm^2 heat flows in the area.

Integrating all the results and deductions obtained in this work, it can be deduce that those regions with shallow or low sedimentary thicknesses (such as Baro, Kutaeregi, Kutiwenji and Koton-karif) are possible areas associated with magnetic mineral ore deposits like oolitic iron ore identified in Koton-Karfi area (Figure 18). Actually, these areas might not support hydrocarbon generation.

However, the sedimentary infillings around Pategi, Agaje, Olle and Baro areas are relatively high in conjunction with the high geothermal gradient and heat flow. It will possibly pave way for hydrocarbon potential in this area provided that all other conditions for hydrocarbon generation are

available. Previous studies such as Adeleye (1974), Okubo et al. (1985), Ojo and Akande (2012) and Bemsen et al. (2013) suggest that the study area contains carbonaceous shale intercalated with sandstone and clay. It is a potential source rock.

8   Conclusions

The qualitative interpretation of the TMI data and residual anomalous data shows a complex configuration of magnetic signatures of the wavelengths. This varying amplitude of the anomalous bodies denotes changes in magnetic intensities from diverse causative sources which is evident in the study area (such as magnetic intensity range between 7200 nT and 8500 nT). Around Paiko, Kutaeregi, Koton-karfi, Bida, Lapai, Agaje, and Aiyegunle areas, the TMI and residual anomalous maps show the magnetic intensities of underlying basement range from 7500 to 8460 nT and -220 to 240 nT, respectively. There are strong evidences of igneous intrusion when juxtaposed with the geologic map of the area. However, at the central parts (Pategi, Baro, Gulu, Lafiagi areas) and beyond, the contour lines are extensively spaced indicating that the sedimentary infilling within these areas is thick. Therefore, we conclude that the widely spaced contours in conjunction with the high magnetic acoustic field intensity values may have been related to the vein bearing

Figure 18. A generalized model for possible mineral deposits and hydrocarbon accumulation.

mineral. This affirmation is reinforced by the geologic information of the study.

The 3D structural model shows the presence of uplifts and depressions, a characteristic manifestation of secondary structural feature named folds. Lineament alignment in the area was produced from the residual anomalous magnetic data. The main structural trends were NE-SW with minor E-W and NW-SE trends. Juxtaposing these lineaments on the geological area shows high concentration of structural lineaments in the area with intense tectonic activities believed to be due to intrusive igneous bodies and the less concentrated areas fall around zone of high sedimentary infillings suggesting deeply seated basement rock.

The structural configuration of the study area is in conformity with the trend of structures within the basin with trends NE-SW and NNE-SSW as prominent trends, and E-W, NW-SE, and W-E as the minor trends. Previous studies have established that NE-SW, NNE-SSW and NW-SE trends within the study area are as a result of Pan-African Orogeny, while the E-W trend may perhaps be as a result of Pre-

Pan-African Orogeny.

Quantitative result revealed two depth models. In the shallower model, seated anomaly varied from 0.56 to 1.96 km for Peter's slope method, and from 1.27 to 1.96 km for spectral analysis. The depth of deeper bodies varies from 2.01 to 3.27 km for Peter's slope method, while for spectral analysis it varies from 2.01 to 4.27 km. However, the depth to the centroid obtained through the spectral analysis ranges from 9.79 to 15.75 km across the study area. The depths to the top of magnetic anomalies obtained through spectral analysis were used to identify the prevalent intrusive bodies along the magnetic profiles. This result is in conformity with earlier works done within Nupe Basin and portions of the adjoining basement. The northeastern and southern parts of the study area have evidence of huge igneous intrusions. It is believed that the basement rocks of the central Nigeria might have intruded within and around the study area.

Furthermore, the model map of depth to the centroid reveals higher depth values at areas like Kutiwenji, Egbako, Lapai, Paiko, Baro, Mopa and Olle, while lower

values are recorded at Lafiagi, Isanlu-Esa, Gulu and Abaji. The 3-D surface plot of the Curie isotherm depth shows the presence of peaks (uplifts) and depressions (troughs) across the study area. Around Kutiwenji, Egbako, Lapai, Paiko, Baro, Mopa, Agaje, and Olle areas, there are visible linear depressions and these areas reveal higher depth to the Curie point isotherm than the other parts such as Lafiagi, Isanlu-Esa, Gulu and Abaji areas which have prevalent uplifts (peaks) in conjunction with lower values. At the northern and southern axes (Kutiwenji, Kutaeregi, Paiko, Lapai, Egbako, Mapo, and Olle), the geothermal gradient thickness is lower compared to the other areas (Figure 16). At Lafiagi Isanlu-Esa, Egbe, Abaji and Gulu areas, geothermal gradient has relatively high geothermal gradient ranging between 25.76 and 30.95°C/km with an average of 25.27°C/km.

Core sample analysis within some parts of the study area reveals that depth to top of the oolitic iron ore across the area ranges from 20.79 to 101.2 m with an average of 38.52 m. Thus, maps of the oolitic iron ore levels with respect to elevations were generated in order to depict the possibly trend of the oolitic iron ore level across the study area. It is predominantly in NE-SW direction and the mineralization will follow this trend.

In this study, we were able to delineate the basin configuration of the region through the interpretation of magnetic and core drilling datasets. A structural model that reveals the geometry of the region is outlined. Again, the present study was able to identify regions containing magmatic intrusions that should be avoided when searching for hydrocarbons. Additionally, in this study, a model was developed to easily identify potential areas of magnetic deposits and hydrocarbon accumulation.

Acknowledgments

References

Abraham, E. M., Lawal, K. M., Ekwe A. C., Alile, O., Murana, K. A., and Lawal, A. A., 2014, Spectral analysis of aeromagnetic data for geothermal energy investigation of Ikogosi Warm Spring-Ekiti state, Southwestern Nigeria: Geothermal Energy, **26**, 1-21.

Abraham, E. M., Onwe, M. R., Ojonugwa, U. A., Gwazah, C. A., and Uchenna, M. E., 2022, Mapping of mineral deposits within granitic rocks by aeromagnetic data—a case study from Northern Nigeria: Arabian Journal of Geosciences, **15**, 1656.

Adeleye, D. R., 1974, Sedimentology of the fluvial Bida Sandstone (Cretaceous), Nigeria: Sedimentary Geology, **12**(1), 1-24.

Adewumi, T., Salako, K. A., Alhassan, U. D., Adetona, A. A., Abdulwaheed, R. A., and Udensi, E. E., 2021, Interpretation of airborne radiometric data for possible hydrocarbon presence over Bornu basin and its environs, Northeast Nigeria using Thorium normalisation method: Iranian Journal of Earth Sciences, **13**(3), 161-172.

Akande, S. O., Ojo, O. J., and Ladipo, K. O., 2005, Upper Cretaceous sequences in the Southern Bida Basin, Nigeria: Mosuro Publishers, Ibadan, Nigeria.

Anakwuba, E. K., and Chinwuko, A. I., 2015, One dimensional spectral analysis and Curie depth isotherm of Eastern Chad Basin, Nigeria: Journal of Natural Sciences Research, **5**(19), 14-22.

Bemsen, I. E., Godwin, O. A., Kenechukwu, A. E., Ifeanyi, C. A., and Ojonugwa, U. A., 2023, Evaluation of geothermal energy potential of parts of the Middle Benue trough Nigeria: aeromagnetic and aeroradiometric approach: Iranian Journal of Geophysics,

16(4), 7-52.

Bemsen, I. E., Onwuemesi, A. G., Anakwuba, E. K., Chinwuko, A. I., Ojonugwa, U. A., and Okonkwo, C. C., 2013, Spectral analysis of aeromagnetic data over part of the Southern Bida basin, West-Central Nigeria: International Journal of Fundamental Physical Sciences, **3**(2), 27-31.

Bhattacharryya, B. K., and Leu, L. K., 1975, Spectral analysis of gravity and magnetic anomalies due two dimensional structures: Geophysics, **40**, 993-1031.

Biswas, A., 2015, Interpretation of residual gravity anomaly caused by a simple shaped body using very fast simulated annealing global optimization: Geoscience Frontiers, **6**(6), 875-893.

Biswas, A., and Acharya, T., 2016, A very fast simulated annealing method for inversion of magnetic anomaly over semi-infinite vertical rod-type structure: Modeling Earth Systems and Environment, **2**(4), 1-10.

Biswas, A., Parija, M. P., and Kumar, S., 2017, Global nonlinear optimization for the interpretation of source parameters from total gradient of gravity and magnetic anomalies caused by thin dyke: Annals of Geophysics, **60**(2), G0218, 1-17.

Chinwuko, A. I., Ojonugwa, U. A., Onwuemesi, A. G., Anakwuba, E. K., Okonkwo, C. C., and Ikumbur, E. B., 2014, Interpretations of aeromagnetic data over Lokoja and environs, Nigeria: International Journal of Advanced Geosciences, **2**(2), 66-71.

Chinwuko, A. I., Onwuemesi, A. G., Anakwuba, E. K., Onuba, L. N., and Nwokeabia, N. C., 2012, The interpretation of aeromagnetic anomalies over parts of Upper Benue Trough and Southern Chad Basin, Nigeria: Advances in Applied Science Research, **3**(3), 1757-1766.

Mandal, A., Biswas, A., Mittal, S., Mohanty, W. K., Sharma, S. P., Sengupta, D., Sen, J., and Bhatt, A. K., 2013, Geophysical anomalies associated with uranium mineralization from Beldih mine, South Purulia Shear Zone, India: Journal Geological Society of India, **82**(6), 601-606.

Obaje, N. G. J., Balogu, D. O., Idris-Nda, A., et al., 2013, Preliminary integrated hydrocarbon prospectively evaluation of the Bida Basin in North Central Nigeria: Petroleum Technology Development Journal, **3**(2), 36-65.

Ojo, O. J., and Akande, S. O., 2012, Sedimentary facies relationships and depositional environments of the Maastrichtian Enagi Formation, Northern Bida Basin, Nigeria: Journal of Geography and Geology, **4**(1), 136-147.

Ojonugwa, U. A., Ezeh, C. C., and Chinwuko, I. A., 2018, Integration of aeromagnetic interpretation and induced polarization methods in delineating mineral deposits and basement configuration within Southern Bida Basin, North-West Nigeria: Journal of Geology & Geophysics, **7**, 1-13, doi: 10.4172/2381-8719.1000449.

Okonkwo, C. C., Onwuemesi, A. G., Anakwuba, E. K., Chinwuko, A. I., Bemsen, I. E., and Ojonugwa, U. A., 2012, Aeromagnetic interpretation over Maiduguri and environs of Southern Chad Basin, Nigeria: Journal of Earth Sciences and Geotechnical Engineering, **2**(3), 77-93.

Okubo, Y. J., Graf, R., Hansen, R. O., Ogawa, K., and Tsu, H., 1985, Curie point depth of the Island of Kyushu and surrounding areas, Japan: Geophysics, **53**, 481-491.

Olufemi, O. A., Yinka, A. M., Alao, E. I., and Alexander, A. F., 2020, Magnetic rocks distribution and depth to basement analysis on an old quarry site, Abeokuta, SW Nigeria: Iranian Journal of Earth Sciences, **12**(3), 176-183.

Onwuemesi, A. G., 1995, Interpretation of magnetic anomalies from the Anambra Basin of Southeastern Nigeria: Ph.D

thesis, Nnamdi Azikiwe University Awka, Nigeria.

Onwuemesi, A. G., 1997, One dimensional spectral analysis of aeromagnetic anomalies and Curie depth isotherm in the Anambra Basin of Nigeria: Journal of Geodynamics, **23**(2), 95-107.

Ross, H. E., Blakely, R. J., and Zoback, M. D., 2006, Testing the use of aeromagnetic data for the determination of Curie depth in California: Geophysics, **71**(5), 51–59.

Saibi, H., Aboud, E., and Azizi, M., 2015, Curie point depth map for Western Afghanistan deduced from the analysis of aeromagnetic data: Proceedings World Geothermal Congress 2015, Melbourne, Australia, 19-25.

Singh, A., and Biswas, A., 2016, Application of global particle swarm optimization for inversion of residual gravity anomalies over geological bodies with idealized geometries: Natural Resources Research, **25**(3), 297-314.